

A study of the Rieger-type period asymmetry in the northern and southern hemispheres during the 19-23 solar activity cycles

Xuan Lu¹

¹Student, College of Communication Engineering, Chengdu University of Information Technology, Chengdu 610225, China; 2

Date of Submission: 10-10-2023

Date of Acceptance: 20-10-2023

ABSTRACT: There are many statistics about the asymmetry of the Northern and Southern hemispheres. In this paper, we study the sunspot area and sunspot number of the solar activity cycles from 19 to 23 solar activity cycles. The extraction of Rieger-type periods for the solar northern and southern hemispheres is carried out by synchrosqueezed wavelet transform (SSWT) and wavelet analysis (WT), respectively. Afterwards, the mean period scales of Rieger cycles of the corresponding activity cycles are obtained by the fitting method and global wavelet analysis, respectively. From there, the asymmetry of the mean period of Rieger-type periods on the northern and southern hemispheres scales is comparatively analyzed.

KEYWORDS: SSWT, wavelet analysis, solar activity, Northern and Southern hemisphere asymmetry.

I. INTRODUCTION

The activity of the sun can be presented in various ways, such as solar flares, sunspots, solar prominences, etc. It has been shown that Rieger-type periods are found among the different activity indices of many solar periods^[1], that their origin is the complex dynamics of the solar interior, and that the Rieger-type cycles are associated with solar activity at stronger periodicities. The intensity of solar activity is usually asymmetric between the northern and southern hemispheres^[2], which may indicate a similar behavior in Rieger-type periods. Previous articles identified Rieger period in the range of 150-185 days^[3]. We analyzed the sunspot data during the 19-23 solar active cycles and extracted the period components using SSWT and

WT, which have different values in the northern and southern hemispheres, thus the Rieger-type periods has a north-south asymmetry in the sunspot region. The study of Rieger period not only provides statistical information about solar flares and control mechanisms, but also has important significance for the spatial and temporal evolution of magnetic phenomena in the subphotospheric layer. In addition, sunspots have a close relationship with auroras, crop yields, and telecommunication communications on the Earth, and the prediction of future trends in solar activity through the study of the activity patterns of sunspots in the northern and southern hemispheres can effectively improve our way of life.

II. SSWT AND WT

CWT can also handle such signals, but its resolution is weak due to the Heisenberg uncertainty principle, and the results obtained are not satisfactory when reconstructing complex signals. And the simultaneous compression wavelet transform as a high-resolution time-frequency transform.

For a signal $x(t)$ containing white noise, its wavelet coefficients can be expressed as:

$$W_x(a, b) = a^{-1/2} \int_{-\infty}^{\infty} x(t) \psi^* \left(\frac{t-b}{a} \right) dt \quad (1)$$

when both the scale a and the value of the time offset b are real, $W_x(a, b)$ can be obtained from Equation (1) as the wavelet coefficients of the original signal $x(t)$. Also a suitable mother wavelet $\psi(t)$ needs to be chosen for processing the signal. The $\psi^*(t)$ is the conjugate complex of $\psi(t)$. Then, the instantaneous frequency of the original signal is estimated by equation (2).

$$\omega_x(a, b) = -i(W_x(a, b))^{-1} \frac{\partial}{\partial b} W_x(a, b) \quad (2)$$

Then a time domain to frequency domain transformation is performed[4]. In performing the SST, the wavelet coefficients are calculated from the k_{th} value a_k in the time domain. ω_1 is the central angular frequency in the interval $[\omega_1 - 1/2 \cdot \omega, \omega_1 + 1/2 \cdot \omega]$. $T_x(\omega_1, b)$ in the interval can be expressed by ω_1 , which leads to:

$$T_x(\omega_1, b) = (\Delta\omega)^{-1} \sum_{a_k} W_x(a_k, b) a_k^{-3/2} (\Delta a)_k \quad (3)$$

where $(\Delta a)_k = a_k - a_{k-1}$, $\Delta\omega = \omega_1 - \omega_{1-1}$, and $a_k = |\omega_x(a_k, b) - \omega_1| \leq \Delta\omega/2$.

The reconstructed signal is then obtained by inverse wavelet transform:

$$\begin{cases} x(t) = \mathcal{R}e[C_\psi^{-1} \sum_l T_x(\omega_l, t) \Delta\omega] \\ C_\psi = \frac{1}{2} \int_0^\infty \hat{\psi}^*(\xi) \frac{d\xi}{\xi} \end{cases} \quad (4)$$

where $\hat{\psi}(\xi)$ is the Fourier transform of the mother wavelet $\psi(t)$, and C_ψ is the normalization constant [5].

WT is becoming a common tool for analyzing local variations in power within time series. By decomposing the time series into time-frequency space, one is able to identify dominant patterns of variability and how these patterns change over time. In this paper, WT was used to find rieger-type time

scales in two data series. Global wavelets are performed to obtain the average periodic scale.

The steps of WT usually include the following:

1. wavelet transform: the original signal or data is subjected to a wavelet transform to decompose it into wavelet components on different scales and frequencies.
2. Power Spectrum Estimation: Calculate the power spectrum for each wavelet component to determine the contribution of different frequency components
3. Scale Spectrum Estimation: Estimates the spectral properties at different scales to reveal the scale dependence of the signal or data.
4. phase spectrum analysis: analyze the phase relationship between different frequency components to understand the temporal relationship between them.

III. EXPERIMENTATION

In terms of data selection, we conducted a comparison experiment by comparing the solar period extracted from two data: daily sunspot area and sunspot number. The two data sources are (1) the daily sunspot area of the Royal Observatory of Greenwich for 1874-2016 and (2) the daily sunspot number data of the Royal Observatory of Belgium for 1874-2016.

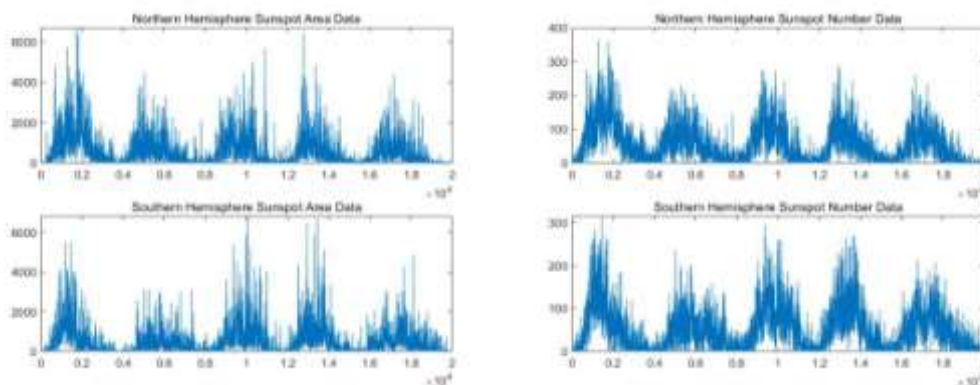


Fig.1 Sunspot data (sunspot area data on the left, sunspot number data on the right; northern hemisphere above and southern hemisphere below).

Since we know a priori that the rieger period is around 150 to 180 days, we perform band interval screening of the raw sunspot data by SSWT. Considering that the SSWT algorithm has a certain error in screening the frequency band, and that the rieger period signal is not completely

within the interval of 150~180, we selected the frequency screening interval between 0.004~0.01HZ, which corresponds to the period of 100~250 days. The signal extraction of the raw data by SSWT yields the northern and southern hemisphere rieger signals as in Fig. 2:

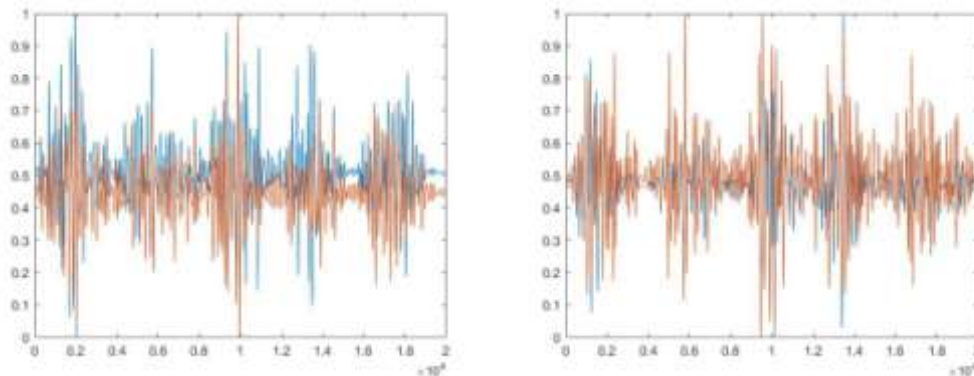


Fig.2 SSWT extracted rieger signals (sunspot area data on the left and sunspot number data on the right; where blue indicates the northern hemisphere and red the southern hemisphere.)

The obtained rieger signals are then segmented according to the corresponding solar activity cycles, and the rieger signals of 19~23

solar activity cycles are obtained, respectively, as shown in Fig. 3:

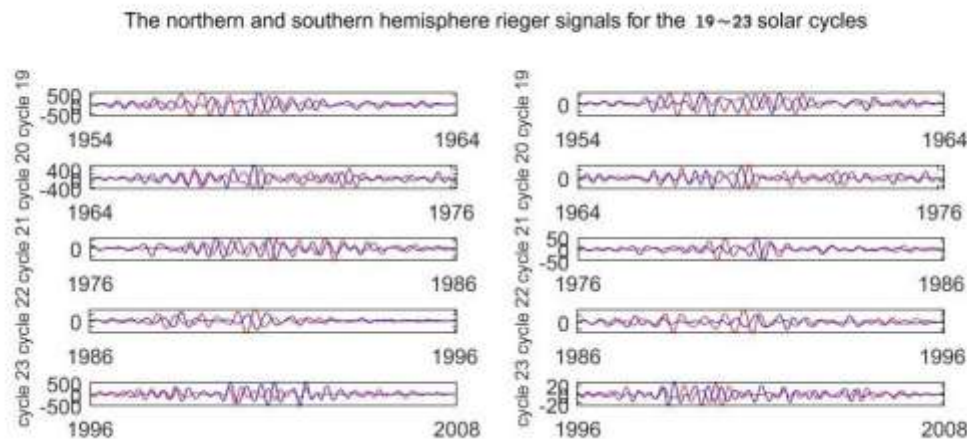


Fig.3 19~23 solar activity cycles southern and northern hemisphere rieger signals (sunspot area data on the left, sunspot number data on the right; where blue represents the northern hemisphere and red represents the southern hemisphere.)

The extracted rieger signals are then fitted, the signals are Hilbert transformed to obtain the corresponding instantaneous frequencies, and then the anomalies caused by Nyquist noise are deleted, and the resulting instantaneous frequencies are subjected to a probability density distribution, and ultimately Gaussian fitting is performed, and the

highest point of the fit is the average period of the weekly rieger period of the solar activity cycle.

The resulting fitted image of the mean period obtained from the rieger signal for the northern and southern hemispheres is shown in Figure 4 below:

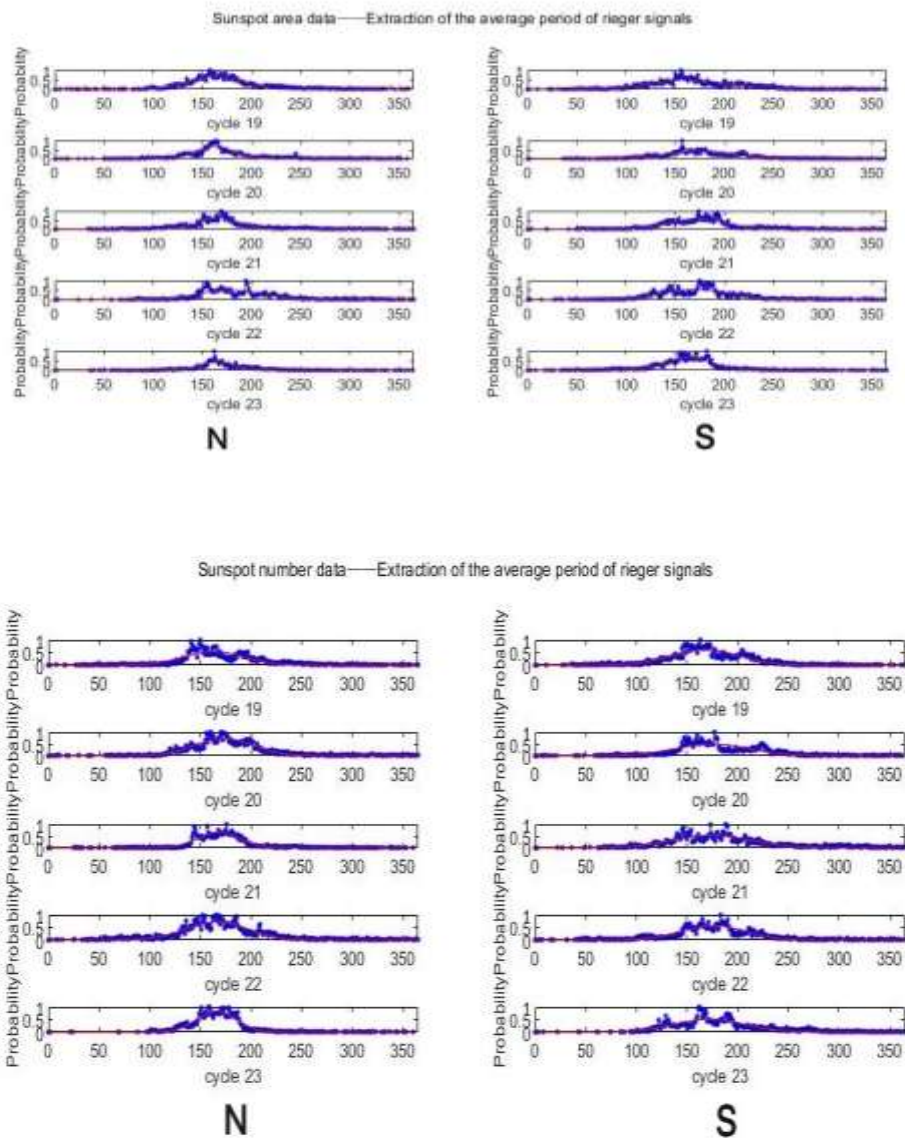


Fig.4 Fitted image of the instantaneous frequency of the rieger signal (sunsport area data above, sunspot number data below; where the left is the northern hemisphere and the right is the southern hemisphere)

Compared to earlier intelligent algorithms such as EMD [6], SSWT is not affected by the uncertainty principle and has anti aliasing and anti noise capabilities.

WT is a mathematical technique used to analyze and process signals, images and data. It was first proposed by Torrance and Compo in 1998 and is primarily used to analyze data in the field of marine and atmospheric sciences in order to better understand climate and weather patterns. This analytical method combines the features of wavelet analysis and spectral analysis and can be used to

study the time and frequency characteristics of signals and data. The main idea of WT is to decompose a signal or data into wavelet components on different scales (or frequencies) in order to better understand its variations over time and frequency. This type of analysis can help identify periodicities and trends in a signal, as well as fluctuations on different scales.

WT of the solar data was performed to obtain Figures 5, 6, 7, and 8:

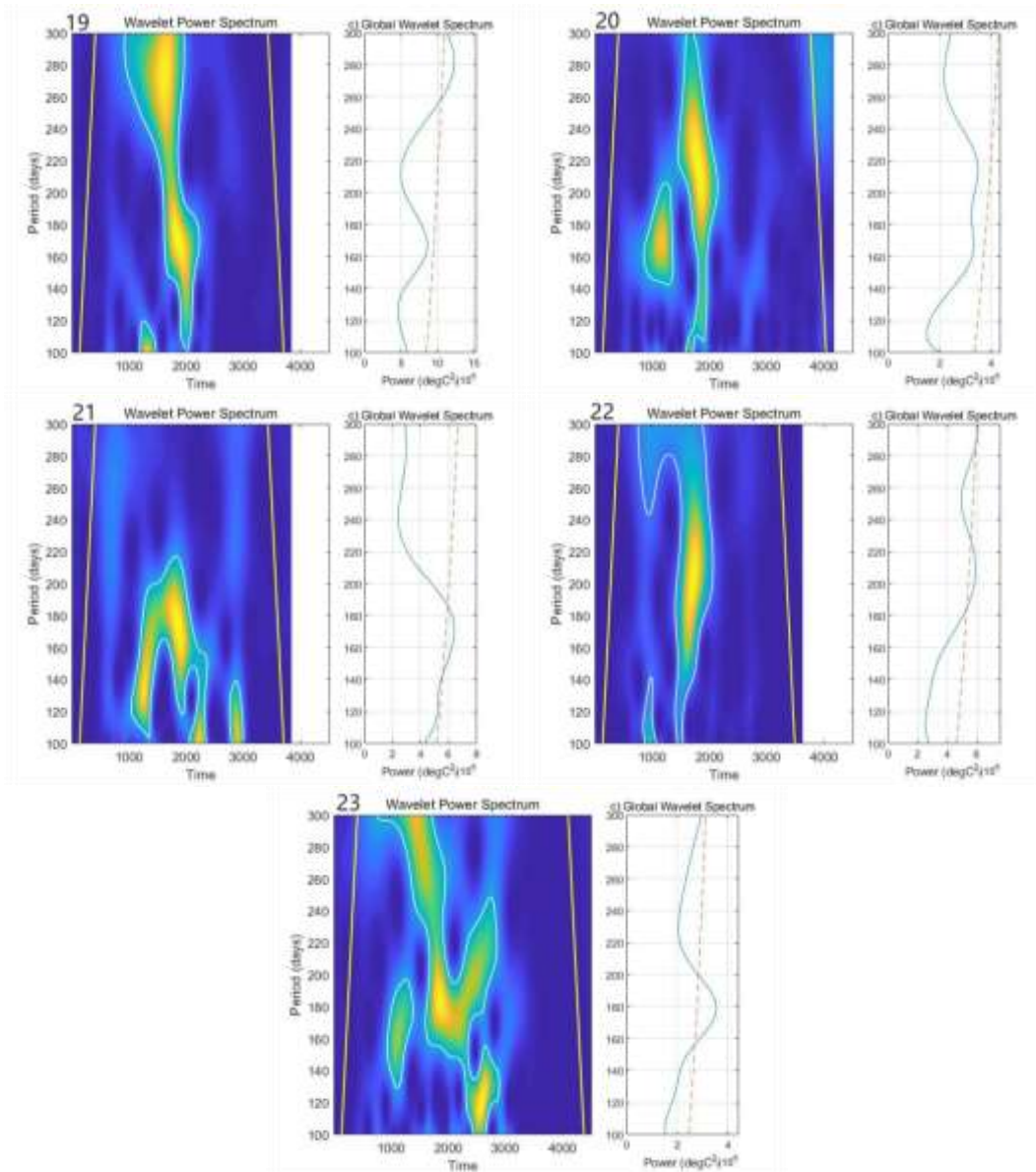
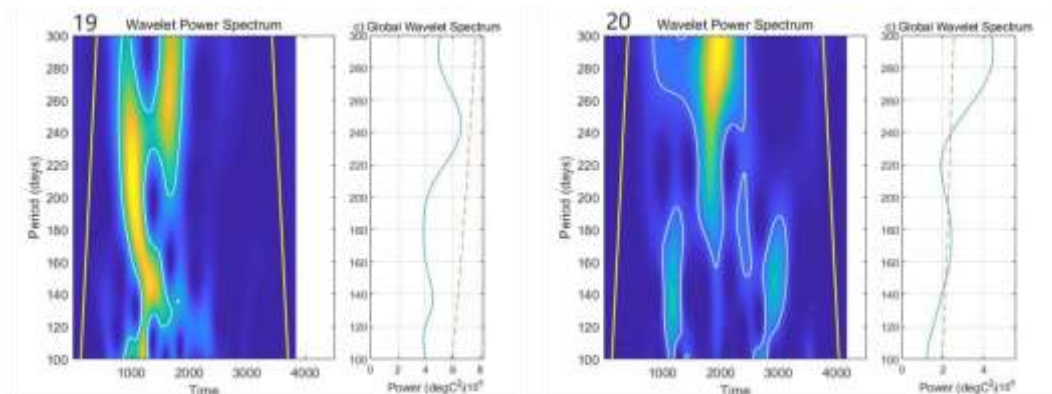


Fig.5 Global wavelet analysis of northern hemisphere sunspot area data for wavelet analysis during the 19-23 solar activity cycles.



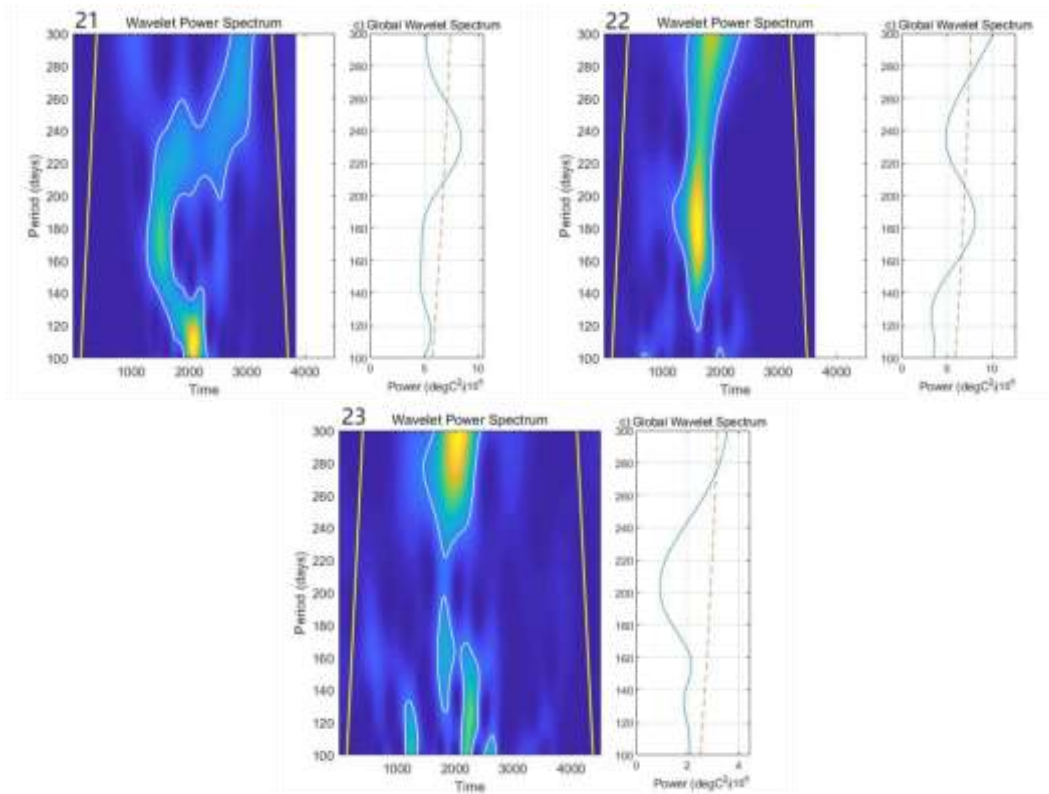
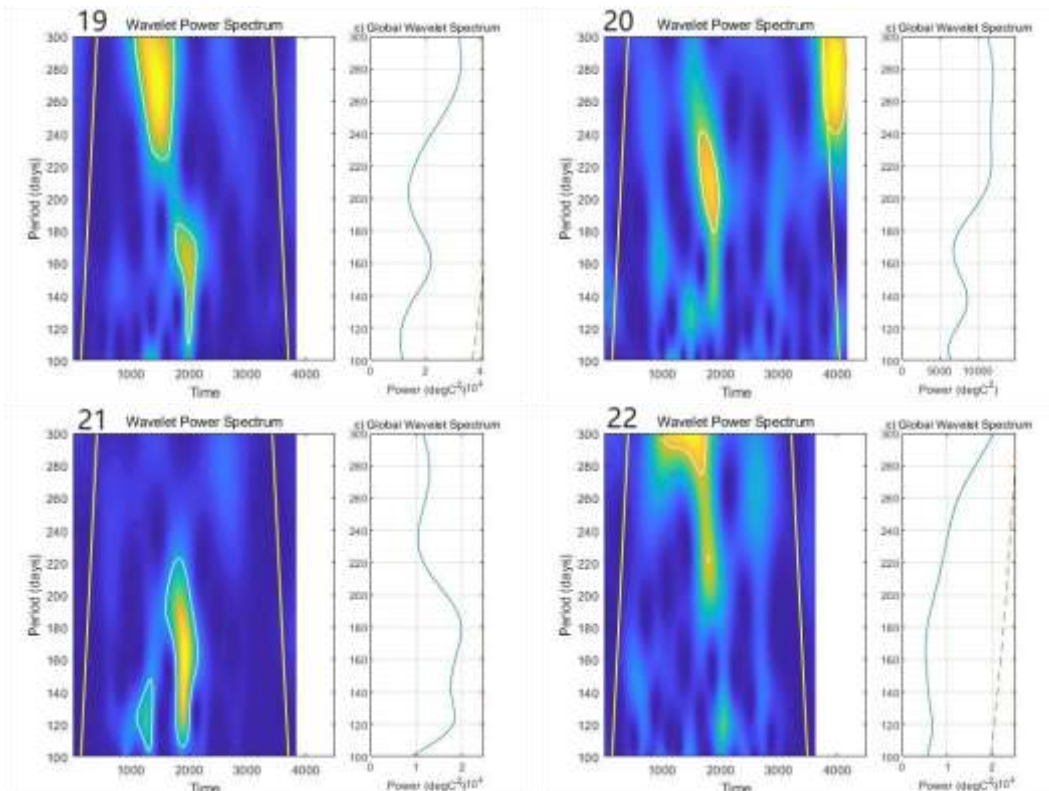


Fig.6 Global wavelet analysis of southern hemisphere sunspot area data for wavelet analysis during the 19-23 solar activity cycles.



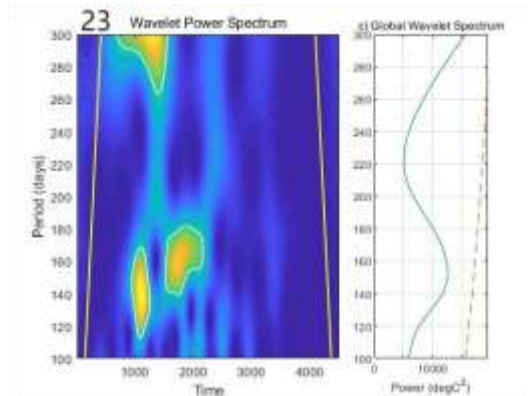


Fig.7 Global wavelet analysis of northern hemisphere sunspot number data for wavelet analysis during the 19-23 solar activity cycles.

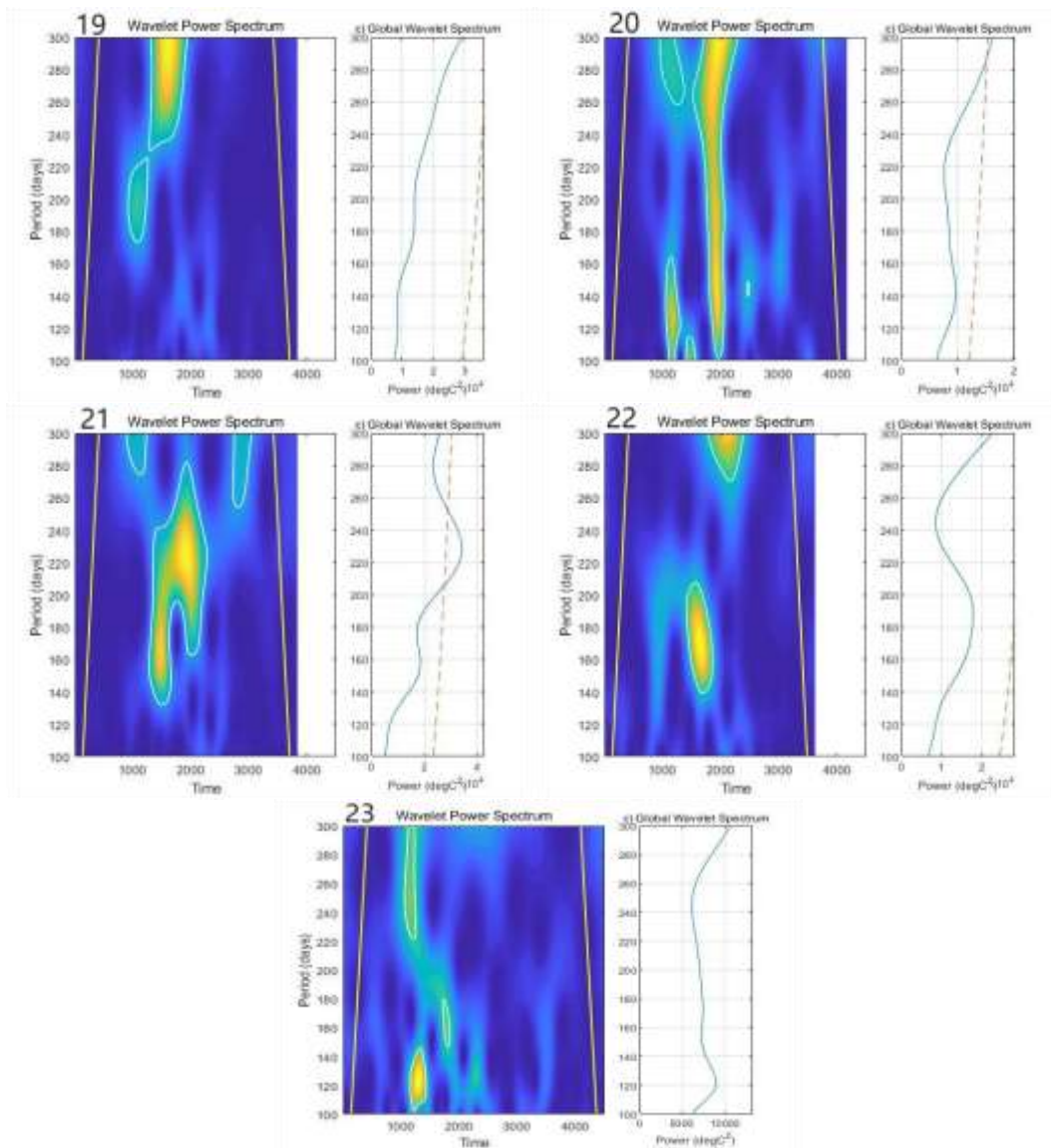


Fig.8 Global wavelet analysis of southern hemisphere sunspot number data for wavelet analysis during the 19-23 solar activity cycles.

The average period of the rieger signals in the northern and southern hemispheres obtained from SSWT and WT were counted to obtain the following Table 1:

Tab.1 The average period of the rieger signals

Average period	SSWT				WT			
	SSA		SSN		SSA		SSN	
Cycle	N	S	N	S	N	S	N	S
19	165	164	162	164	166	138	159	179
20	162	171	173	170	164	173	137	189
21	167	173	168	178	171	166	179	158
22	179	172	167	168	208	184	-	181
23	166	163	166	175	179	146	151	173

IV. CONCLUSION

As can be seen from Table 1, both sunspot area and sunspot number are characterized by rieger signals, while their extracted period scales will have different conclusions with different extraction methods.

In the 19th, 21st, and 23rd solar weeks, the average period scales of the rieger cycles in the northern and southern hemispheres extracted from the sunspot area data and the sunspot number data by SSWT do not differ much, but the rieger signals extracted from the two data in the 20th and 22nd solar weeks are somewhat different.

WT has some limitations when extracting the mean period of rieger signals. Although wavelet analysis can effectively extract features from complex multi-frequency astronomical signals. However, its extraction of the mean period may be affected by the combined effect of the relatively weak circumferential magnetic field and torsional oscillations [7], resulting in localized analyses where the rieger period does not exist in some solar activity cycles. For example, the northern hemisphere sunspot number data for the 22th active cycle, whereas SSWT has the advantage over wavelet analysis for feature extraction in that it can accommodate a wide range of signal types, including both periodic and non-periodic signals, and is more stable. WT has significant differences in the processing of the two

data, which is a limitation of WT itself.

REFERENCES

- [1]. Rieger E, Share G H, Forrest D J, et al. A 154-day periodicity in the occurrence of hard solar flares?[J]. Nature, 1984, 312(5995): 623-625.
- [2]. Cowling T G. The stability of gaseous stars[J]. Monthly Notices of the Royal Astronomical Society, 1934, 94: 768-782.
- [3]. Chowdhury P, Choudhary D P, Gosain S, et al. Short-term periodicities in interplanetary, geomagnetic and solar phenomena during solar cycle 24[J]. Astrophysics and Space Science, 2015, 356: 7-18
- [4]. Daubechies I, Lu J, Wu H T. Synchrosqueezed wavelet transforms: An empirical mode decomposition-like tool[J]. Applied and computational harmonic analysis, 2011, 30(2): 243-261.
- [5]. Thakur G, Brevdo E, Fućkar N S, et al. The synchrosqueezing algorithm for time-varying spectral analysis: Robustness properties and new paleoclimate applications[J]. Signal Processing, 2013, 93(5): 1079-1094.
- [6]. Liu Weixing, Mode Decomposition Study on the Area Changes of Sunspots in the Northern and Southern Hemispheres of the Sun Based on EMD [D] two thousand and nineteen.
- [7]. Xiang N B, Zhao X H, Li F Y. Publ. Astron. Soc. Aust, 2021, 38: e032